Cement and Concrete Research 39 (2009) 787–797

Contents lists available at ScienceDirect

Cement and Concrete Research

journal homepage: http://ees.elsevier.com/CEMCON/default.asp

Characterising the time-dependant behaviour on the single fibre level of SHCC: Part 2: The rate effects on fibre pull-out tests

William P. Boshoff [a,*], Viktor Mechtcherine [b], Gideon P.A.G. van Zijl [a,c]

[a] Division for Structural Engineering, University of Stellenbosch, Private Bag X1, Stellenbosch, South Africa
[b] Faculty of Civil Engineering, Technical University Dresden, Germany
[c] Faculty of Architecture, Delft University of Technology, The Netherlands

ARTICLE INFO

Article history:
Received 1 June 2008
Accepted 8 June 2009

Keywords:
Fibre reinforcement
Pull-out strength
Tensile properties
Rate effects
SHCC

ABSTRACT

This paper is the second part of a two paper series about the time-dependant behaviour of Strain Hardening Cement-based Composite (SHCC) on the single fibre level. Having dealt with mechanisms of creep in SHCC in the first part, this paper reports single fibre pull-out tests that were done to investigate the effect of the pull-out rate on the mechanical response of the interface between the fibre and the matrix. It was found that not only the pull-out resistance increased with an increase of the pull-out rate but the probability of fibre rupture during pull-out as well. Another important finding was that the interfacial shear resistance and slip-hardening coefficient are not only dependant on the pull-out rate, but also the embedment length.

1. Introduction

SHCC (Strain Hardening Cement-based Composite) is a class of high performance fibre-reinforced cement composites which has been developed for pseudo strain-hardening, or increased tensile resistance beyond first cracking, over a significant tensile deformation, in some cases more than 4% [1–3]). The pseudo strain-hardening is due to effective bridging of the cracks by fibres, whereby multiple, fine cracks form under tensile loading. This superior tensile behaviour is achieved by engineering the matrix, fibres and the fibre–matrix interface to achieve an optimum behaviour using less than 2.5% of fibre by volume [4,5].

Another important benefit of this material is the durability improvement. Relatively large cracks may arise in ordinary reinforced concrete (RC), which lead to durability concerns for the steel reinforcement. SHCC, on the other hand, can produce fine multiple cracking with a crack width less than 60 μm [2] at large tensile deformation, which reduces water and chloride penetration rates to several orders of magnitude lower than those for crack widths beyond 0.1–0.2 mm, usually accepted in RC. Therefore an increased durability of a SHCC structure can be expected as compared to RC.

Before the use of a new building material such as SHCC, the time-dependant behaviour requires investigation to enable reliable structural use of the material. The creep and creep fracture of the material are likely to cause failure at a load lower than the static ultimate load. The ductility could also be reduced when the material is exposed to a sustained load for a long period of time. The rate dependence may include composite embrittlement under increased loading rate by mobilisation of a different failure mechanism. The strain-hardening deformation range may be reduced due to fibre breakage rather than fibre pull-out. To shed light on these causes of concern, the sources of the time-dependant behaviour of SHCC should be studied and understood. Here, the focus is on the rate dependence.

In recent years, a number of research reports have been published about the rate dependence on the macro level [6,7,8,3]. These tests were done by varying the imposed strain rate in uni-axial tensile tests. Significant trends are:

- All authors showed that the stress at first cracking increased with an increase of the strain rate, except for Maalej et al. [6] who did not report the first cracking strength. Boshoff and Van Zijl [3] quantified the increase as 70% over strain rate increase of 4 orders of magnitude.
- All authors showed that the (ultimate) tensile strength, which is controlled by the fibres bridging the cracks, has an increase of more than 70% except for Boshoff and Van Zijl [3] who showed an increase of only 17%.
- Yang and Li [7] and Douglas and Billington [8] reported a decrease in tensile strain capacity of more than 50% with an increase of the strain rate. However, Maleej et al. [6] and Boshoff and van Zijl [3] showed no significant change in the strain capacity within their tested strain rate regimes.

In the above reported experimental programs different fibres, matrix compositions and dimensions of the test specimens contribute to the conflicting results. Nevertheless, it is postulated that the fibre–matrix interaction governs the described phenomena of rate-dependent behaviour. To comprehend the tensile rate dependence

* Corresponding author.
E-mail address: bboshoff@sun.ac.za (W.P. Boshoff).

0008-8846/$ – see front matter © 2009 Elsevier Ltd. All rights reserved.
doi:10.1016/j.cemconres.2009.06.006

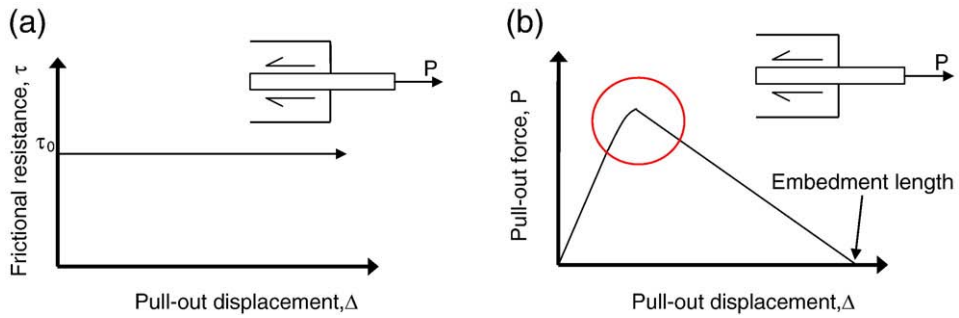

Fig. 1. (a) The uniform shear resistance model for fibre pull-out. (b) The fibre pull-out response using this model is shown schematically.

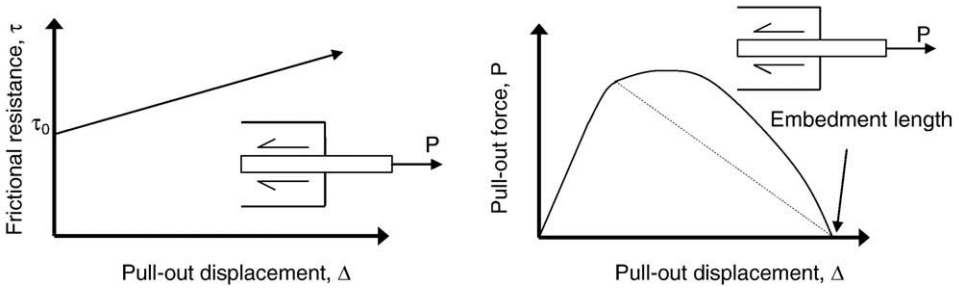

Fig. 2. The effect of the slip-hardening coefficient on the interfacial shear resistance between the fibre and the matrix is shown schematically.

of SHCC and illuminate the role of fibre–matrix interaction, an investigation is required on the meso-level, i.e. the single fibre level. On this level, sources of the time-dependant behaviour can be identified and understood. This paper reports on rate tests that were done on the single fibre level. Fibres that were embedded in the matrix were pulled out at different loading rates and the applicable fibre–matrix interface parameters were derived. This was done to find the effect of the loading rate on the parameters and to understand this source of time dependence. A Scanning Electron Microscopy (SEM) investigation was also performed on the interface to gain further insight in the cause of the time dependence.

2. Analytical single fibre pull-out models

In SHCC as in any FRC, three structural components exist, which are the matrix, the fibres and the matrix–fibre interface. To be able to design the material for the desired SHCC mechanical behaviour the single fibre pull-out behaviour must be understood and mathematically modelled. To study this behaviour, as well as the rate and time dependence, it is useful to consider analytical models of fibre–matrix interaction. For this purpose, micro-mechanical models commonly used for the description of the fibre pull-out behaviour are briefly described in this section.

The most basic model of the fibre pull-out behaviour was introduced by Li [4] for the use in micro-mechanical modelling of SHCC. The model is based on the assumption that a spatially uniform frictional traction is present on the surface between the fibre and the matrix during pull-out. The magnitude of the frictional shear traction is given as τ_0 and the model is shown schematically in Fig. 1a. This model also assumes that the value of τ_0 is the same regardless of the embedment length of the fibre and is independent of the pull-out displacement. This model would result in a fibre pull-out response as shown schematically in Fig. 1b. Note that the nonlinearity in the ascending branch is due to gradual debonding.

An adjustment was made to this model by Lin and Li [9] by introducing a slip-hardening coefficient, β. A model that included slip-hardening was needed to consider the phenomenon that the interfacial bond, τ_0, increases as the pull-out displacement increases.

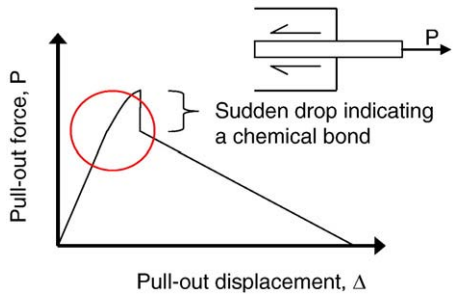

Fig. 3. The sudden drop of pull-out force that indicates that a chemical bond exists between the matrix and the fibre is shown schematically.

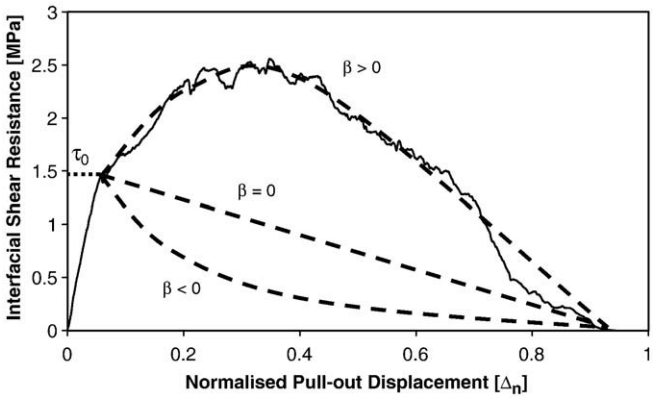

Fig. 4. The approximation of β and τ_0 is shown graphically.

Table 1
Single fibre embedment length pull-out tests.

	Embedment length tests			
Number of specimens	5	5	5	5
Embedment length [mm]	1.0 to 1.5	1.5 to 2	4	6

The effect of the pull-out displacement on the interfacial shear resistance if slip-hardening is present is shown schematically in Fig. 2 and the expression for τ is given by Eq. (1):

$$\tau = \tau_0\left(1 + \beta\frac{\Delta}{d}\right) \tag{1}$$

with Δ the pull-out displacement and d the fibre diameter.

When PVA (Polyvinyl Alcohol) fibres were introduced to SHCC, a third parameter became necessary to model the fibre pull-out behaviour, termed chemical bond by Kanda and Li [10] and Lin et al. [11]. During the pull-out of fibres which have a high chemical bond or adhesion to the matrix, the bond has to be broken before pull-out can start. This is associated with a sudden load drop after full debonding of the fibre, as shown schematically in Fig. 3. This load drop is caused by the unstable debonding which occurs if the force required to debond the fibre is higher than the frictional resistance after debonding.

Three approaches are available to consider the chemical bond in the micro-mechanical models, namely a strength based model [10], fracture based model [10] and an energy based model [11]. The most widely used model currently for SHCC is the energy based model. The expression to calculate the energy based chemical bond is according to Eq. (2):

$$G_d = \frac{2P_\Delta^2}{\pi^2 E_f d^3} \tag{2}$$

with G_d the chemical bond (i.e. the measure of the energy release due to the loss of the chemical bond), P_Δ the magnitude of the unstable load drop and E_f the stiffness of the fibre.

Keeping these models in mind, single fibre tests were performed and interpreted in this work to study rate and time dependence, as described in the next sections.

3. Experimental setup and method of interpretation

3.1. Test setup

All tests were done using the same mix proportions, namely a water/binder ratio of 0.4 and an aggregate/binder ratio of 0.5. The binder consisted of CEM I 42.5 cement, a fly ash marketed as PozzFill by Ash Resources, South Africa, and Corex Slag of origin of the Saldanha Steel Refinery in the Western Cape Province, South Africa used in the ratio of 45:50:5 by mass respectively. A fine sand of particle size less than 0.2 mm was used as the aggregate. Note that the rheology refinement was achieved by the addition of a super plasticiser and a viscosity modification agent. All specimens were tested at an age of 14 days.

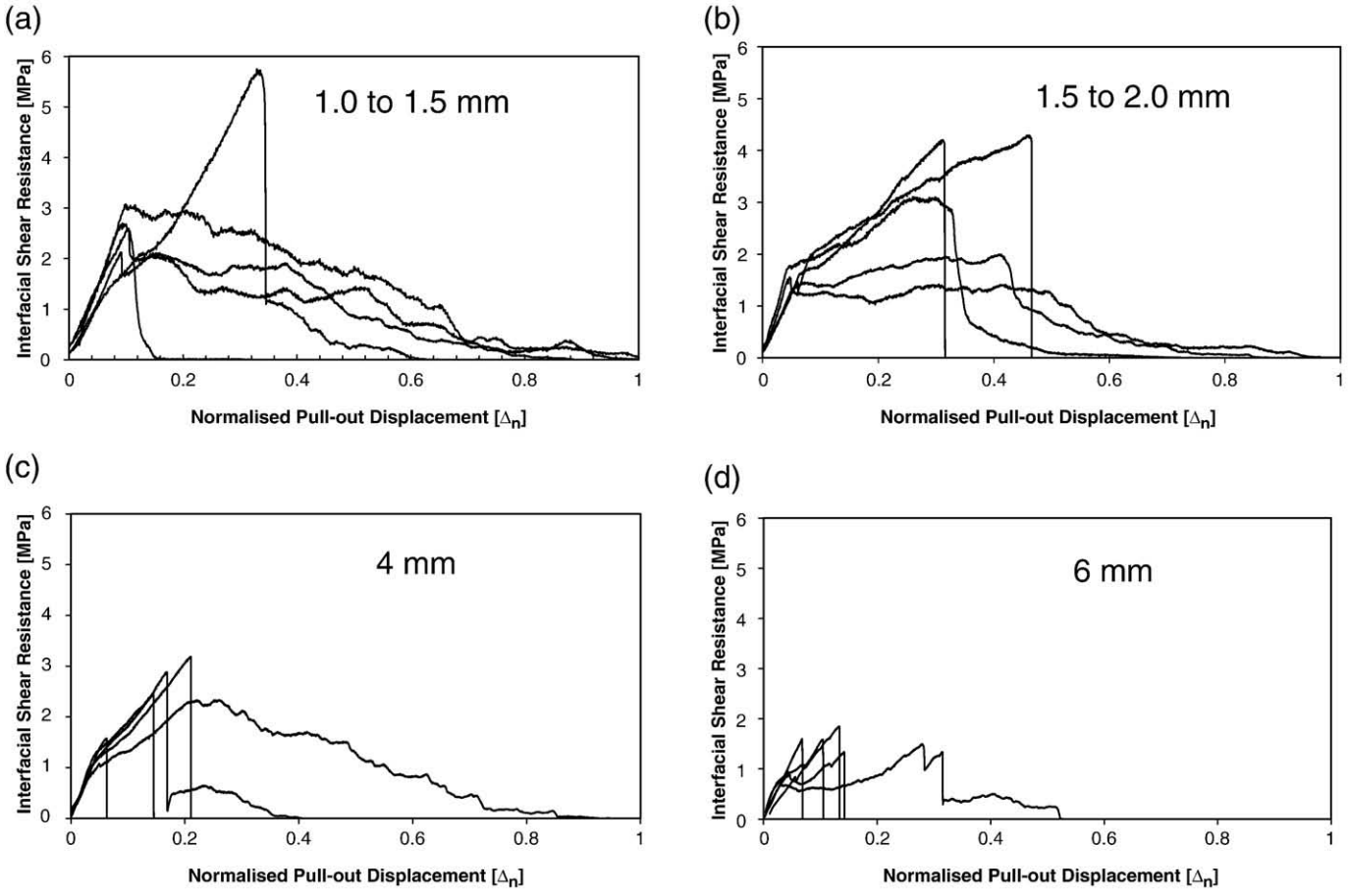

Fig. 5. The results of the embedment length fibre pull-out tests with the specific embedment lengths are shown.

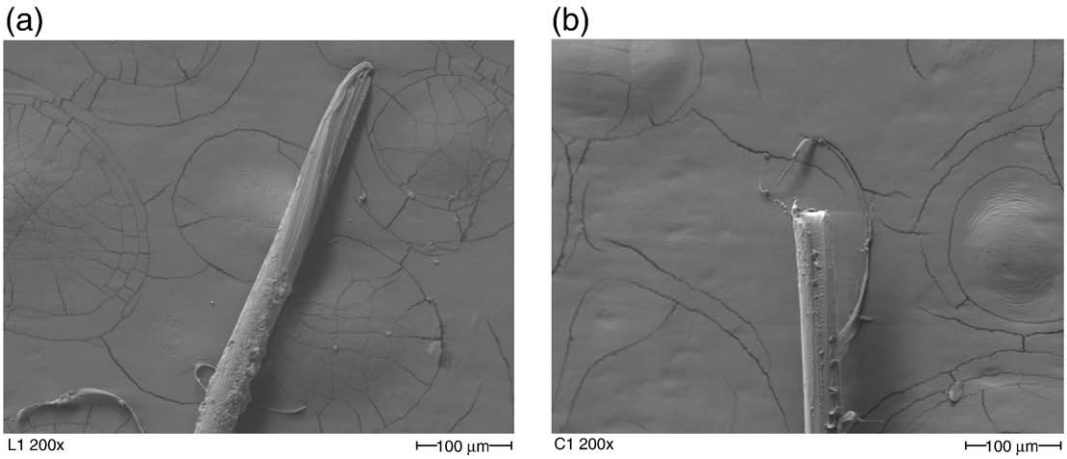

Fig. 6. (a) A SEM photo of a ruptured fibre. (b) A SEM photo of a completely pulled out fibre.

The mould design and the casting procedure of the specimens are based on the work of Katz and Li [12]. The experimental setup is described in detail in the accompanying paper, Boshoff et al. [13].

3.2. Method of interpretation

Slight differences of the embedment length cause large variations of the pull-out displacements and forces, it means the results had to be normalised for comparison. For this, the force was expressed as a shear stress and the displacement of the pull-out tests was normalised.

The model of a uniformly distributed shear resistance along the embedment length of the fibre is assumed. All the force readings are expressed as an interfacial shear resistance by dividing it by the surface area of the embedded fibre that is in contact with the matrix using Eq. (3):

$$\tau = \frac{P}{L_e \pi d} \tag{3}$$

with P the applied force, d the fibre diameter and L_e the original embedment length.

The normalised displacement Δ_n, calculated according to Eq. (4):

$$\Delta_n = \frac{\Delta}{L_e} \tag{4}$$

with Δ the measured displacement during the pull-out test, should equal 1.0 when complete pull-out is achieved.

The slip-hardening/slip-softening coefficient, β, is calculated from Eq. (1) with a positive β representing slip-hardening and a negative β slip-softening. β is found by doing an individual curve fitting exercise with every result using Eq. (1), to find the most appropriate β. A typical result is shown in Fig. 4 with the method of approximation of τ_0 and β represented graphically.

However, before the pull-out rate tests could be performed, embedment length tests were required as decision had to be made at what embedment length the rate tests were to be done. For this, single fibre pull-out tests were carried out at different embedment lengths to determine which embedment length should be used.

4. Embedment length tests

4.1. Test program

Embedment length tests were performed to assist in choosing an embedment length for the single fibre pull-out rate tests. These tests were also used to investigate the effect of the embedment length on the interface parameters. A standard pull-out rate of 1 mm/min was used. The test program is summarised in Table 1.

4.2. Test results

The results of the embedment fibre length tests are shown in Fig. 5. The force and the displacements are normalised as described above. The range of the axes is the same for all the graphs to ease the comparison. Significant scatter is seen in the test results. This is attributed mainly to different modes of failure (which were either complete fibre pull-out, or fibre rupture) and differences in embedment lengths within the distinguished ranges, but also to inherent variation in matrix heterogeneities.

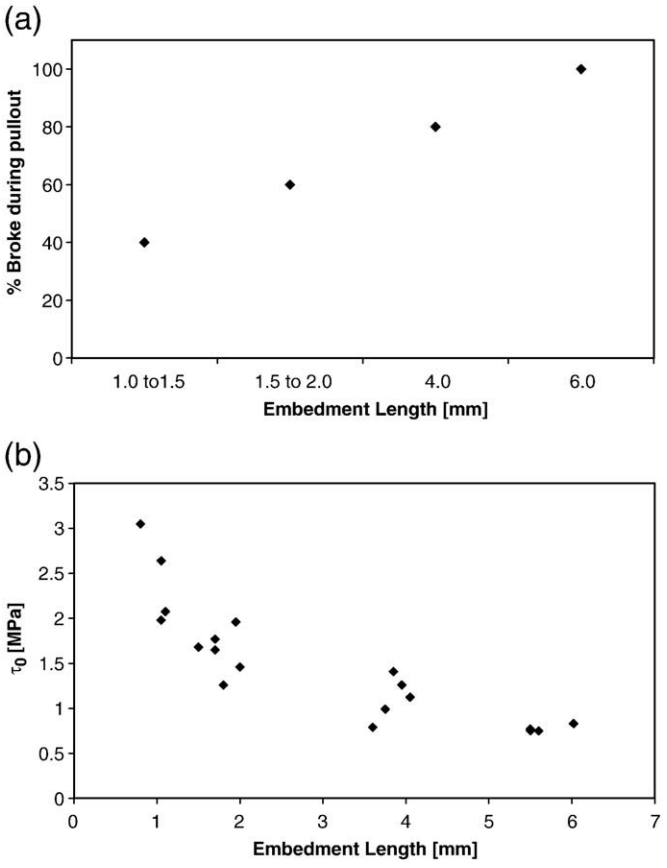

Fig. 7. (a) The percentage of fibres that ruptured during testing versus the embedment length. (b) τ_0 versus the embedment length.

Table 2
Single fibre pull-out rate tests.

	Pull-out rate tests				
Number of specimens	5	4	6	7	4
Embedment length [mm]	Average = 1.39; COV = 16%				
Loading rate [mm/s]	0.01	0.1	1	10	100

As can be seen from the results, not all fibres were pulled out completely as many of them fractured during pull-out. This can be distinguished from the results, because a fibre that ruptures shows a sudden drop of force while the response of a fibre that pulls out completely would show a steady load reduction until a zero load resistance when or just before the normalised pull-out displacement, Δ_n, reaches 1. To confirm this, SEM pictures were taken of the fibre ends that were embedded in the matrix. In Fig. 6a an example is shown of a ruptured fibre end, and in Fig. 6b an example of a fibre that pulled out completely. From the SEM pictures it is clear to distinguish which fibres ruptured and which fibres pulled out completely. The end of the latter fibre shows signs of a mechanical cut edge, which occurred during the preparation of the testing sample as described in the previous section.

4.3. Discussion of results

To show that the probability of fibre rupture is dependant on the embedment length, the amount of fibres that ruptured during testing is expressed as a percentage of the number of fibres tested in the set of a specific embedment length. The results are shown in Fig. 7a where the percentages are expressed against the embedment length. A clear

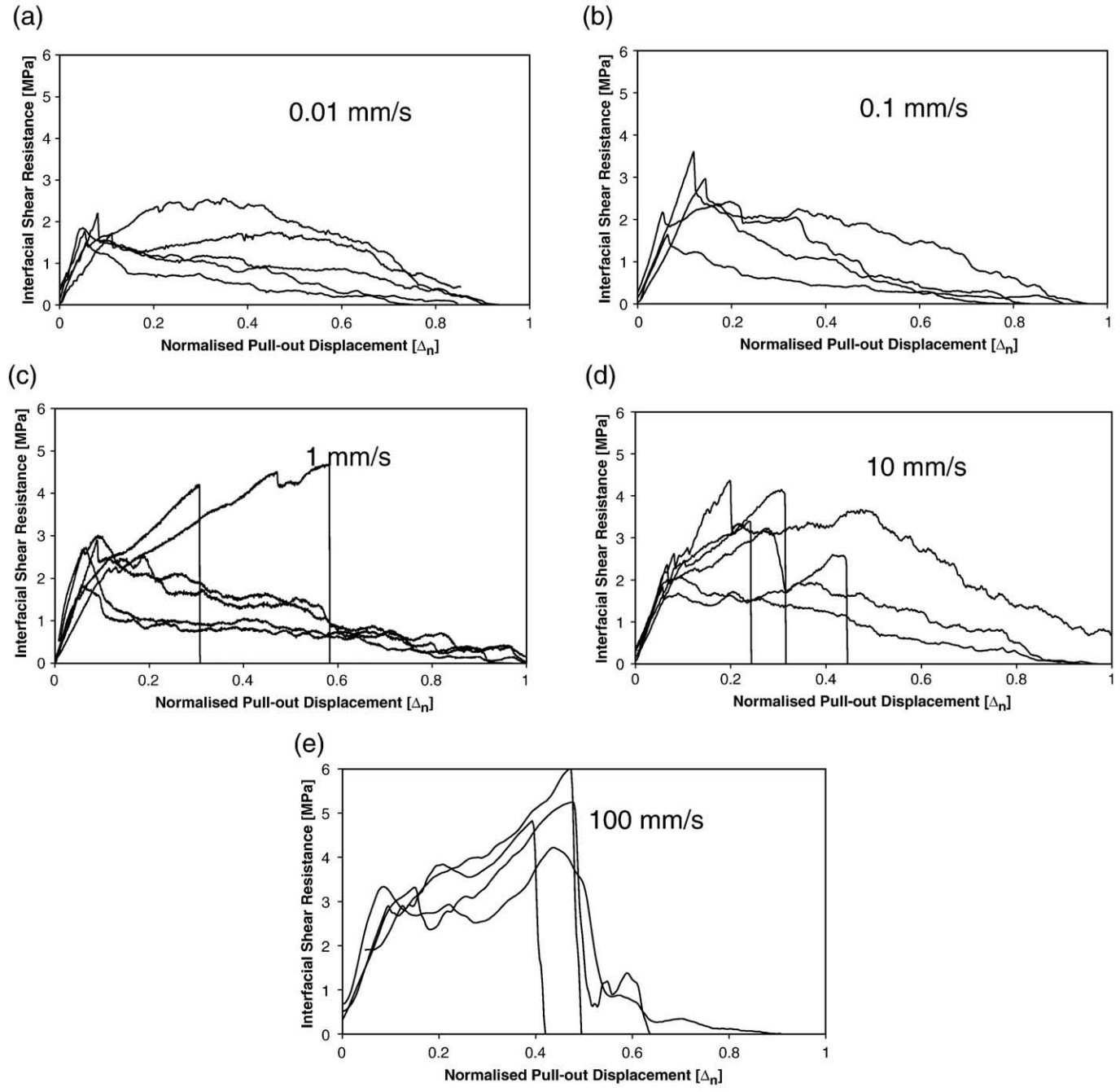

Fig. 8. Results of the single fibre pull-out rate tests with the pull-out rates are shown.

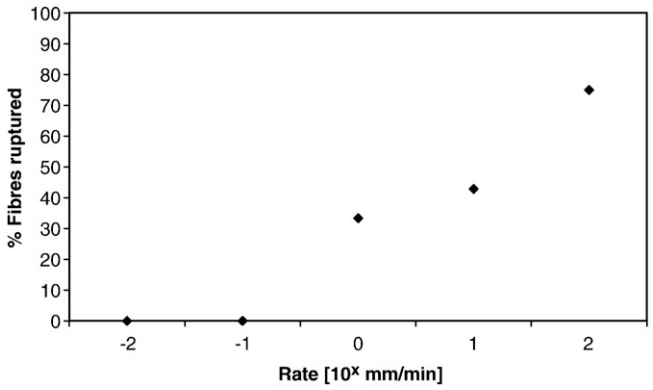

Fig. 9. Percentage of fibres that ruptured during the rate tests expressed against the testing pull-out rate.

dependency of the probability of fibre rupture on the embedment length can be seen, with a higher probability with an increasing embedment length. The initial interfacial shear resistance, τ_0, was found from Eqs. (3) and (1) and is shown in Fig. 7b versus the embedment length.

The chemical bond, G_d, was defined in Eq. (2) as a function of the unstable load drop that occurs during debonding. As shown in Fig. 5, an unstable load drop after debonding was not a regular phenomenon. The G_d will thus be computed as zero for almost all the tests. This may be due to gradual debonding before peak resistance was reached, avoiding a sudden release of the chemical bond energy directly after the peak. Nevertheless, it is assumed that the chemical bond did not play a prominent role in this specific fibre and matrix combination and will for this reason not be derived and discussed.

The primary purpose of these embedment length tests was to establish a suitable embedment length for the single fibre pull-out rate test. For the pull-out tests, the best scenario is when a fibre is pulled out completely as the τ_0 and the β parameters can then be easily identified. As seen in Fig. 7a, the shorter the embedment length, the smaller the chance of fibre rupture, thus the shorter the embedment length, the more suitable the results. However, an embedment length of less than 1 mm is impractical due to the small size of the test sample for preparation and gluing in the test setup. For these reasons an embedment length in the region of 1.4 mm was chosen for the rate tests.

The phenomenon of apparent strength, first identified by Kanda and Li [10], would cause the fibres to fracture at a much lower stress if they are embedded in the matrix in comparison to the ultimate fibre strength of non-embedded fibres. The average strength for the embedded fibre was 959 MPa with a COV of 22.4%. A large COV was to be expected due to the large variation of the type of damage to the fibres that is believed to cause this premature rupture. The apparent strength of the fibres found is 61% of the indicated strength (1560 MPa) of the fibres supplied by Kururay. This corresponds well with the results of Redon et al. [14] that found the apparent strength to be 60% for the same type and almost the same fibre diameter (44 μm compared to 40 μm used in this study).

5. Rate effect on single fibre pull-out behaviour

5.1. Experimental program

Rate tests were performed to investigate the time dependence of the fibre pull-out behaviour. The pull-out rate was varied over four orders of magnitude from 0.01 mm/min to 100 mm/min. The test program is shown in Table 2. The desired embedment length was chosen from the results of the embedment length tests reported in Section 4. To achieve an exact embedment length is hardly possible, which fact is reflected in the variation in embedment length reported in the table.

SEM pictures were also taken of the test samples and the tested fibres to gain insight in the type of damage of the fibres and whether the loading rate had an effect on the damage distribution. The following cases were examined with the SEM:

- The pulled out fibres tested at different pull-out rates as well as an unused fibre as a reference to investigate the effect of the pull-out rate on the damage on the fibre surface.
- The inside of the test sample to find out whether fibres debond and slip before they rupture.
- The inside of the test sample to examine the matrix interface after the fibre has pulled out and the fibres to find possible causes of the slip-hardening phenomenon.

To view the inside of the test samples, the samples were carefully broken open to expose the fibre–matrix interface. This is a difficult process and numerous samples were needed before one was broken in the manner that successfully exposed the interface.

5.2. Test results

The results of the rate tests are shown in Fig. 8 ranging from a pull-out displacement rate of 0.01 mm/min to 100 mm/min. The scaling of the axes of the graphs is the same in order to make the comparison easier. The number of fibres rupturing during the tests is expressed in Fig. 9 as a percentage of the number of fibres tested for each rate.

The results of the rate tests were analyzed and the values of τ_0 and β according to Eqs. (1) and (3) were found and these parameters with regard to the pull-out rate are shown in Fig. 10.

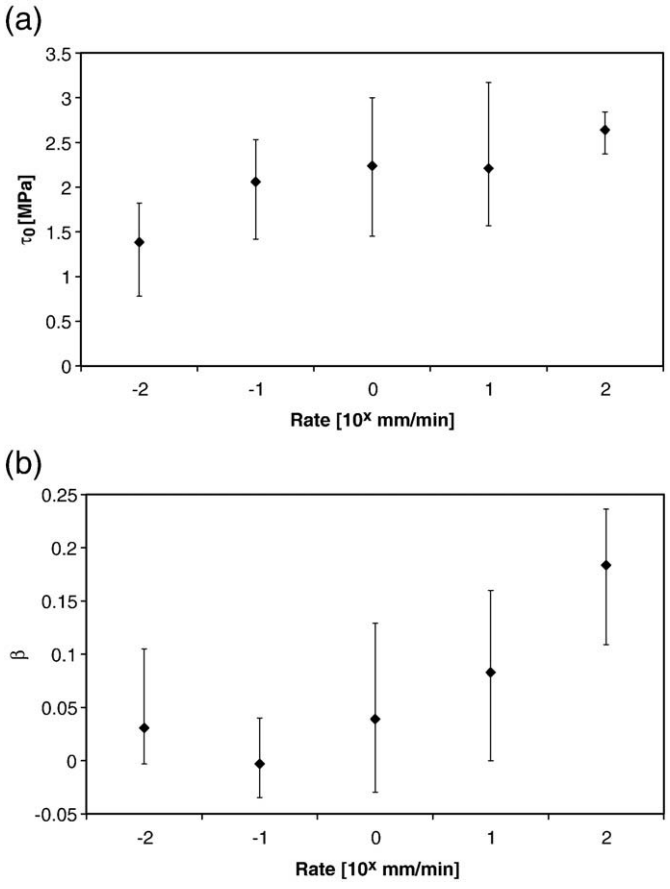

Fig. 10. The range and average values for different pull-out rates with regard to (a) initial interfacial shear resistance, τ_0 and (b) the slip-hardening/softening coefficient β.

5.3. SEM investigation

To see whether the pull-out rate has an influence on the surface damage of the fibres, SEM photos were taken of the pulled out fibres after testing. One typical SEM photo was selected here for each pull-out rate. The photos are shown in Fig. 11 together with a reference fibre that was still unused.

Fig. 11 shows clearly that surface damage occurs during pull-out. The damage is in the form of long, straight scratch marks on the fibres. For the cases when the fibres ruptured during the pull-out tests with very high rates, no part of the fibre that was originally embedded in the matrix could be investigated for surface damage (cf. Fig. 11f). No clear effect could be observed from Fig. 11 on the surface damage of the fibres that can be related to the pull-out rate. This is complicated by the fact that the damage would differ along the fibre length due to different damage patterns and the complex heterogeneity of the matrix. All this makes the exercise of finding a change of the type of the surface damage at different pull-out rates a difficult task if a visual inspection is to be used as a measure.

To verify whether fibre rupture can occur even after full fibre debonding and some slippage has taken place, a SEM picture was taken of the inside of a test sample of which the fibre ruptured during pull-out. This phenomenon would be confirmed if the remaining part of the fibre in the matrix did undergo some slippage, i.e. the end part of the

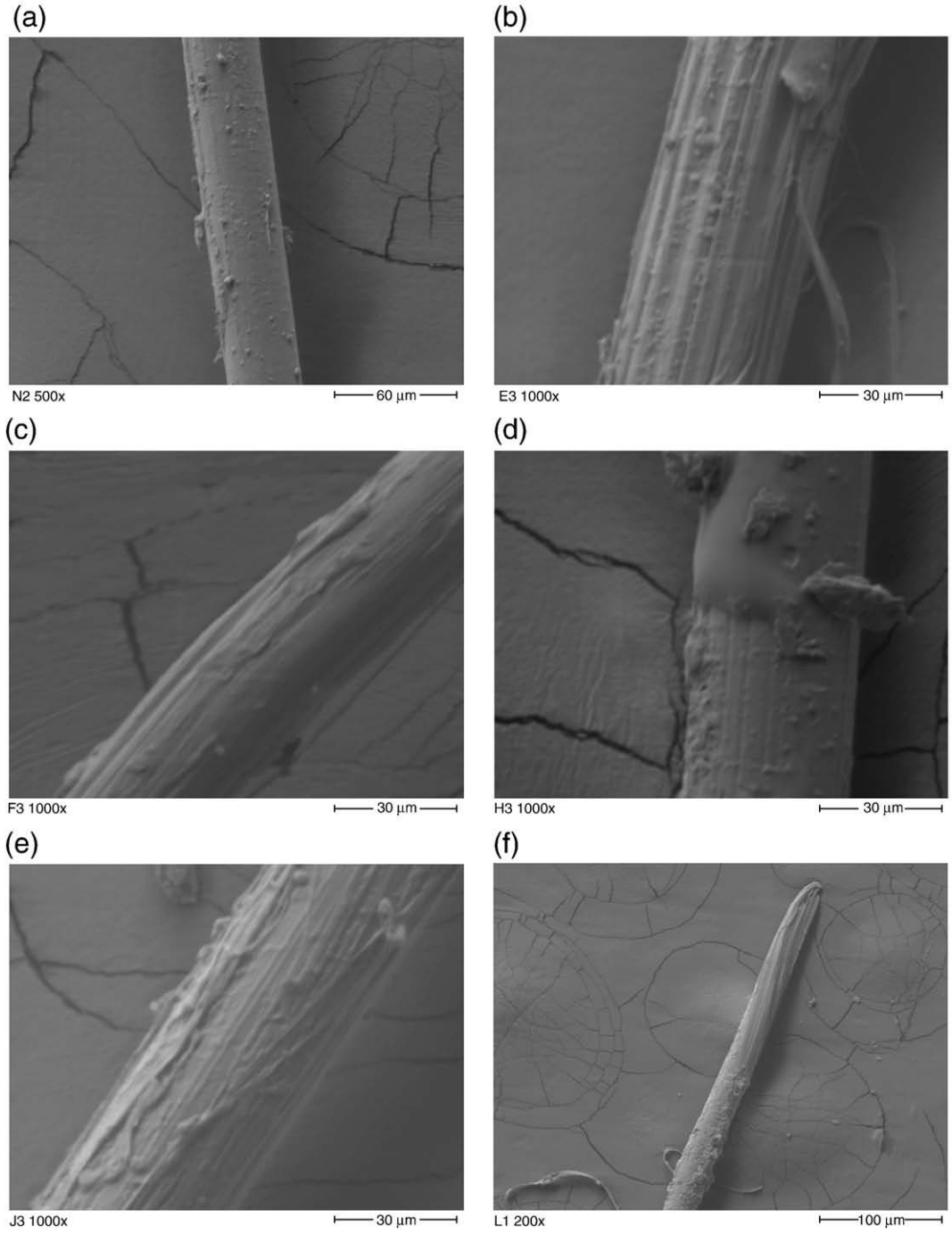

Fig. 11. SEM photo of (a) a reference, unused fibre, and fibres pulled out at the pull-out rate of (b) 0.01 mm/min, (c) 0.1 mm/min, (d) 1 mm/min, (e) 10 mm/min and (f) 100 mm/min.

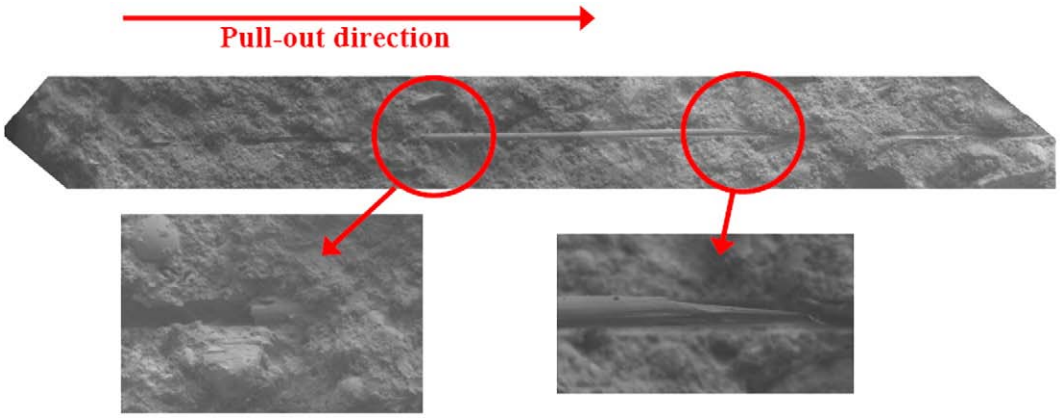

Fig. 12. SEM picture showing the two ends of a fractured fibre that remained in the test sample.

fibre is not in its original position. The SEM pictures in Fig. 12 clearly show this. The remaining part of the fibre has slipped and the end of the embedded side is shown to be the cut end of the fibre and the other end of the fibre still embedded in the sample was clearly ruptured.

To investigate the possible cause of the slip-hardening phenomenon during fibre pull-out, the pulled out fibres were closely inspected to see if strips of fibre were scratched off the surface of the fibre that would cause the damage lines. These strips would get stuck between the fibre and the matrix and would increase the confining pressure and thus increase the frictional resistance. Numerous fibres were found that had loose strands that were still lightly attached to the fibres. This can be seen in Fig. 13. There were also pieces of fibre found left behind in the matrix after complete pull-out as shown in Fig. 14. This clearly indicates that fibre remains that were scratched off the surface during pull-out are one cause of the slip-hardening effect of these pull-out tests, but there is no proof that this is the only cause of slip-hardening.

Based on this theory of slip-hardening, the slip-hardening should also increase with an increase in embedment length as the longer the fibre that has to be pulled-out, the more fibre scrapings would be left behind in the matrix which increase the slip-hardening. An increase of the slip-hardening coefficient with an increase of embedment length

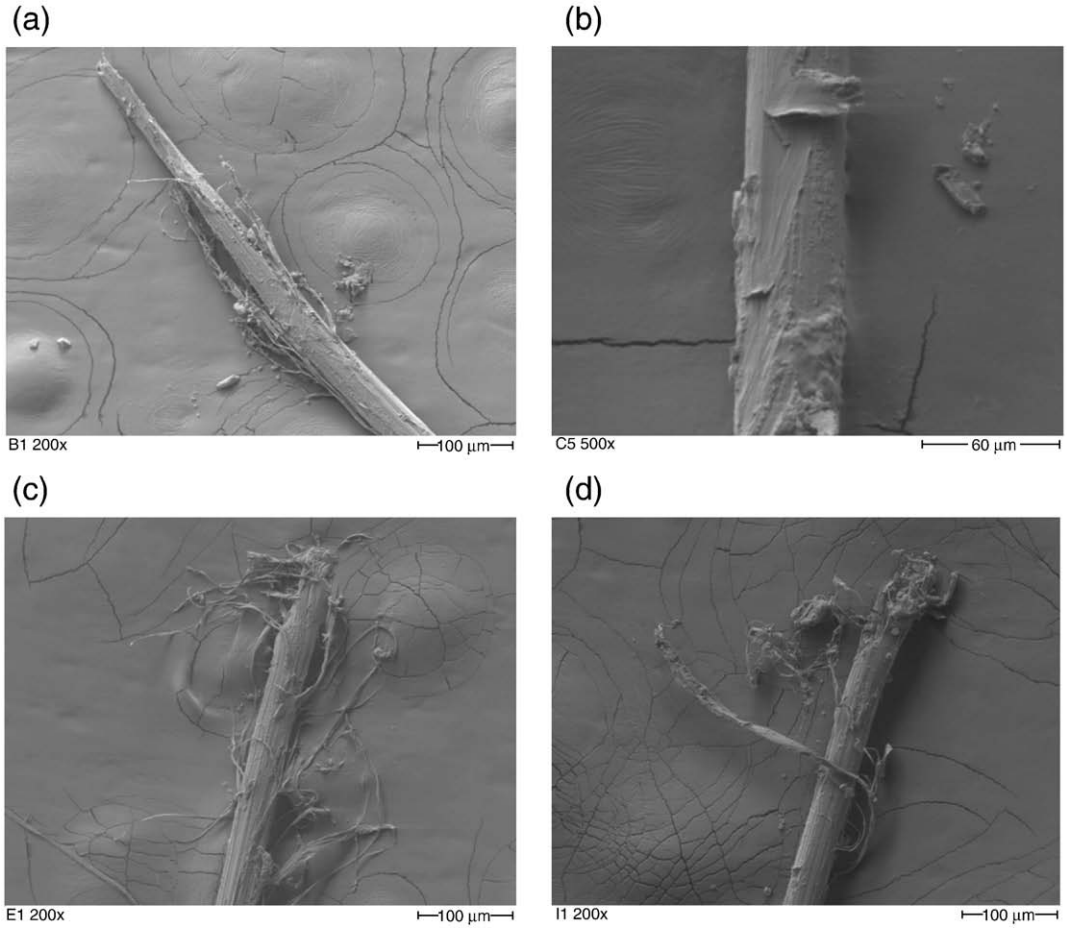

Fig. 13. Surface damage to a pulled out fibre.

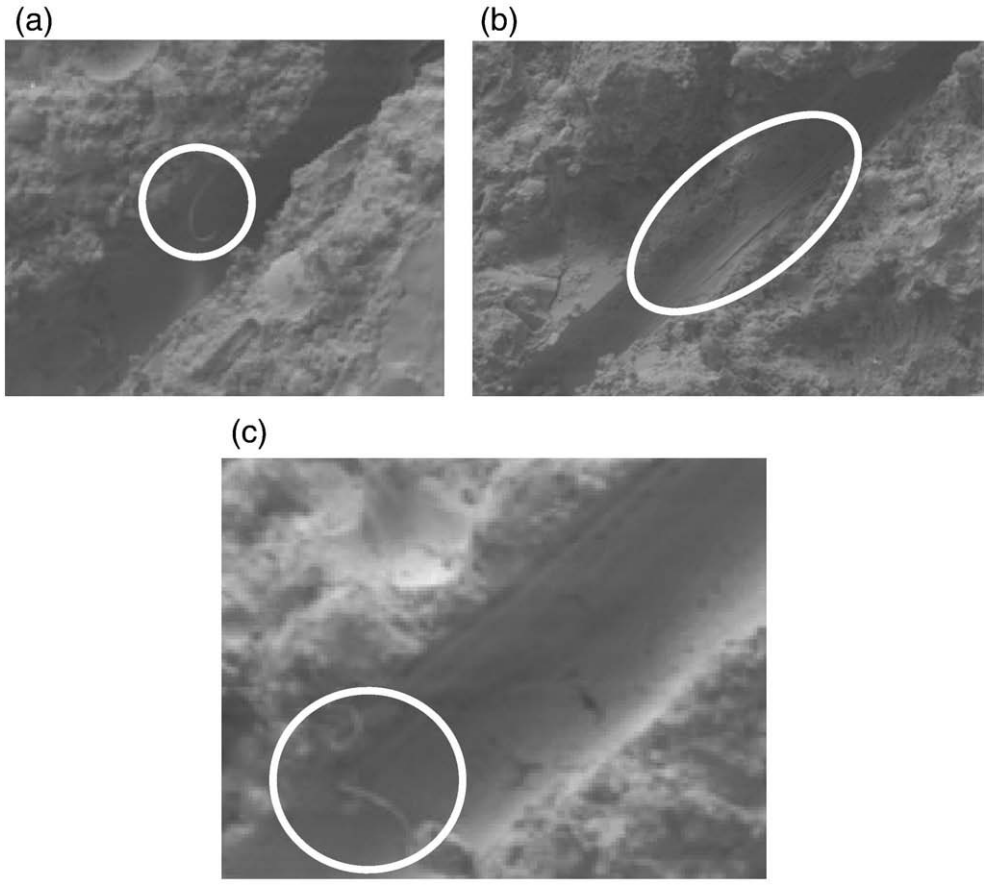

Fig. 14. Signs of remains of fibre in test sample after pull-out.

can be seen in Fig. 5. The curve gradient after debonding gives the indication of the slip-hardening coefficient.

6. Discussion

6.1. Effect of the embedment length

An important phenomenon that was rather unexpected was the reduction of the τ_0 with the longer embedment length, as shown in Fig. 7b. All the micro-mechanical models shown in Section 2 rely on an assumption that the interfacial shear resistance is uniformly distributed along the fibre interface. Fig. 7b clearly shows that this is not the case and the value of τ_0 increases substantially when the embedment length of the test is reduced. The assumption of a uniform distributed shear stress along the embedment length is thus not accurate.

A possible explanation is that the Poisson's ratio of the fibre plays an important role in the distribution of the interfacial shear resistance of the fibre. It has been shown that Poisson's ratio plays an important role in the debonding process of the fibre [15,16] but to the authors' knowledge this has not yet been investigated for the pull-out phase of the fibre. The interfacial shear resistance would reduce if the axial stress in the fibre increases due to the Poisson's ratio effectively reducing the confining pressure which causes the frictional resistance. This is an important phenomenon that requires further investigation. This effect would not play a role in the comparison of the results of the fibre pull-out rate tests as the embedment lengths of these tests were within a relatively small range. This would however cause inaccuracies when the results are used with the micro-mechanical models to simulate the macroscopic behaviour.

Another possible explanation is that for the longer embedment length only a part of it is involved as a result of the gradual stress transfer and partial delamination, while the whole length is used for calculation and evaluation.

The embedment length tests also showed a strong trend that the longer the embedment length, the higher the likelihood of the fibre fracturing during a pull-out test. This phenomenon comes as no surprise, as Redon et al. [14], Lin et al. [11], Kanda and Li [10], Yang and Li [7] and Li et al. [5] all prescribed an embedment length less than 1.2 mm for successful pull-out of a fibre. This value could however vary as the matrix–fibre interface varies with different matrix compositions. A theoretical critical embedment length can be calculated using the model of Lin and Li [9] according to Eq. (5):

$$P = \frac{\pi d_f^2 \tau_0 (1+\eta)}{\omega}\left[\sinh\left(\frac{\omega L}{d_f}\right) - \sinh\left(\frac{\omega(\delta-\delta_0)}{d_f}\right)\right] + \pi\tau_0\beta(1+\eta)(\delta-\delta_0)(L-(\delta-\delta_0)) \tag{5}$$

with

$$\eta = \frac{V_f E_f}{V_m E_m} \tag{6}$$

$$\omega = \sqrt{4(1+\eta)\beta\tau_0 / E_f} \tag{7}$$

$$\delta_0 = \frac{2d_f}{\beta}\left[\cosh\left(\frac{\omega L}{d_f}\right) - 1\right] \tag{8}$$

and d_f the fibre diameter, L the embedment length. V_f and V_m are the volume fractions of the fibre and matrix respectively while E_f and E_m

are the Young's moduli of the fibre and the matrix respectively. P is the pull-out force and δ the pull-out displacement.

Using a value of 960 MPa, the apparent strength for the fibres, $\tau_0 = 2.24$ MPa and $\beta = 0.04$, the values found for the normal testing rate of 1 mm/min, and the critical embedment length can be calculated at 3.0 mm. This value does not correlate with the experimental findings, as about 60% of fibres ruptured with an embedment length less than 2.0 mm. This critical embedment length is however computed using the interfacial parameters calculated from results that had an embedment length around 1.40 mm. The results of this research show that the τ_0 decreases with an increase of embedment length, Fig. 7b. Thus, if the parameters had been obtained for a larger embedment length, a critical embedment length larger than 3.0 mm would be computed. On the other hand, β increases with an increase in embedment length. This would result in a higher than projected pull-out resistance, whereby critical embedment length is effectively reduced.

Note that the apparent strength of the fibres, significantly below its rupture strength when tested separately, can be ascribed to several mechanisms, including (i) crystal growth at the surface acting as notches, (ii) the transition of the soft fibre to the stiff (embedded) fibre which leads to stress concentrations and local failure, and (iii) the fact that a longer embedment length leads to the higher probability of inclusion of weak areas.

6.2. Rate effect

A trend was seen in the fibre pull-out rate tests that showed that the higher the pull-out speed, the higher the probability of fibre rupture. The probability ranged from 0% of fibre rupture at the lowest testing rate to 80% at the highest testing rate. There are not enough test results to show a true statistical probability distribution, but the trend is clear. This is an alarming result as this shows that the fracture mechanism of SHCC may change if the loading rate changes.

The value of initial interfacial shear resistance, τ_0, showed an increase of 91% from the lowest to the highest pull-out rate. This result contradicts the results of Yang and Li [7] who found no influence of rate on the value of τ_0. The embedment length used by Yang and Li [7] was 0.5 mm which is less than half the embedment length used in this study. The embedment length plays an important role in the magnitude of τ_0 as shown in Fig. 7b, and could also influence the mechanism that causes the time-dependant resistance increase and thus possibly explaining the difference found compared to Yang and Li [7]. The value of β increased from around 0 to 0.18 with the increase in pull-out rate. The increase of β is also a trend that was not found by Yang and Li [7] who found no change of β by increasing the pull-out rate. However, their prism test results indicate the likelihood of a change in the mode of fibre failure!

Due to the strong increase of τ_0 and β, it is expected that it would have a compounding effect on the response on the macro level. Using the model of Lin and Li [9], the responses for the average composite crack bridging stress for the lowest, normal and highest test rate are shown in Fig. 15. The respective results for τ_0 and β are used. A strong increase of the ultimate crack bridging stress was found with an increasing pull-out rate using this model, but the rate effect in the tensile tests on the macro level was much less pronounced [3]. This discrepancy can be linked to the apparent trend that at higher pull-out rates, the probability of fibre rupture increases. However, a thorough statistical study, with a larger, statistically significant test sample should be performed to confirm the correctness of this assumption. Fibre rupture is not included in the model of Lin and Li [9]. This could cancel out the effect of the increase of resistance with a higher rate.

From the test results in Figs. 5 and 8 it appears that the fibre rupture occurs at a pull-out displacement of around 0.7 mm for all the pull-out rates. This means that no fibre should rupture at a pull-out displacement of less than 0.7 mm. This is indicated in Fig. 15. Note that this value is a mere reference, to be confirmed with more tests to ensure statistical meaningfulness.

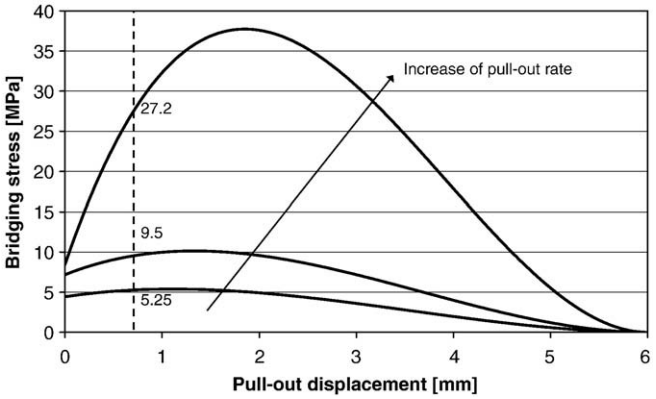

Fig. 15. The crack bridging response with the model of Lin and Li [9] using the interfacial parameters for different pull-out rates.

Theoretically, using this model [9], there should still be an increase of the crack bridging stress from 5.25 MPa to 27.2 MPa on this level. Such strong macroscopic rate effect was not observed on the macroscopic level [3]. It is important to note again that the interfacial parameters used to calculate the responses shown in Fig. 15 were based on pull-out tests with an embedment length around 1.40 mm. β and τ_0 have been shown not to depend only on the fibre and matrix type, but also the embedment length. These effects, together with the inclination of fibres, which was not investigated in the paper, are the reason for the discrepancies with the results of the model of Lin and Li [9]. It must be kept in mind that the gradual debonding and general non-uniform stress transfer complicates analytical modelling.

7. Conclusions

An in depth experimental investigation was done of the time-dependant behaviour on the single fibre level of SHCC. A clear rate effect was found with the pull-out response of the fibres and the results were compared using a slip-hardening pull-out model. The following conclusions can be made:

- A strong increase of peak resistance was found with an increase of loading (displacement) rate in the single fibre tests.
- The probability of fibre rupture increased with an increased loading rate showing that an increased pull-out rate could change the failure mechanism from pull-out to dominantly fibre rupture.
- The strong increase in peak resistance found at higher rates on the single fibre level was not found to this extent on the macro-level. This result can be attributed to the change of the fibre failure mechanism from pull-out to fibre rupture.
- It was shown that the model of uniform distributed shear resistance of fibre is not applicable for the experimental results shown, as the slip-hardening coefficient, β, as well as the interfacial shear resistance, τ_0, derived from the experimental results are dependant on the embedment length.

Acknowledgement

The first author was supported by a DAAD grant. The support of the South African Ministry of Trade and Industry through the Technology and Human Resources for Industry Programme (THRIP), as well as the industrial partners of the THRIP project SAPERCS is gratefully acknowledged.

References

[1] V.C. Li, Engineered cementitious composites — tailored composites through micromechanical modeling, in: N. Banthia, A. Bentur, A. Mufti (Eds.), Fiber Reinforced Concrete: Present and the Future, Canadian Society for Civil Engineering, Montreal, 1998, pp. 64–97.

[2] V.C. Li, S. Wang, C. Wu, Tensile strain-hardening behavior of PVA-ECC, ACI Mater. J. 98 (6) (2001) 483–492.

[3] W.P. Boshoff, G.P.A.G. Van Zijl, Time-dependant response of ECC: characterisation of creep and rate dependence, Cement and Concrete Research, vol. 37, Elsevier, 2007, pp. 725–734.

[4] V.C. Li, Post-crack scaling relations for fiber-reinforced cementitious composties, ASCE J. Mater. Civ. Eng. 4 (1) (1992) 41–57.

[5] V.C. Li, C. Wu, S. Wang, A. Ogawa, T. Saito, Interface tailoring for strain-hardening PVA-ECC, ACI Mater. J. 99 (5) (2002) 463–472.

[6] M. Maalej, S.T. Quek, J. Zhang, Behaviour of hybrid-fibre engineered cemetitious composites subjected to dynamic tensile loading a projectile impact, Journal of Materials in Civil Engineering, ASCE, 2005, pp. 143–152.

[7] E. Yang, V.C. Li, Rate dependence in engineered cementitious composites, Proceedings of HPFRCC RELIM Conference, Hawaii, 2005.

[8] K.S. Douglas, S.L. Billington, Rate dependencies in high-performance fibre-reinforced cement-based composites for seismic application, Proceedings of HPFRCC RILEM Conference, Hawaii, 2005.

[9] Z. Lin, V.C. Li, Crack bridging in fiber reinforced cementitious composites with slip-hardening interfaces, J. Mech. Phys. Solids 45 (5) (1997) 763–787.

[10] T. Kanda, V.C. Li, Interface property and apparent strength of a high strength hydrophilic fiber in cement matrix, ASCE J. Mater. Civ. Eng. 10 (1) (1998) 5–13.

[11] Z. Lin, T. Kanda, V.C. Li, On Interface Property Characterization and Performance of Fiber Reinforced Cementitious Composites, J. Concrete Science and Engineering, vol. 1, RILEM, 1999, pp. 173–184.

[12] A. Katz, V.C. Li, A Special Technique for Determining the Bond Strength of Carbon Fibers in Cement Matrix by Pullout Test, J. Materials Science Letters, vol. 15, 1996, pp. 1821–1823.

[13] W.P. Boshoff, V. Mechtcherine, G.P.A.G. Van Zijl, Characterising the Time-Dependant Behaviour on the Single Fibre Level of SHCC: Part 1: Mechanism of Fibre Pull-out Creep, Cem. Concr. Res. 39 (9) (2009) 779–786.

[14] C. Redon, V.C. Li, C. Wu, H. Hoshiro, T. Saito, A. Ogawa, Measuring and modifying interface properties of PVA fibers in ECC matrix, ASCE J. Mater. Civ. Eng. 13 (6) (2001) 399–406.

[15] Y.C. Gao, Y.M. Mai, B. Cotterell, Fracture of fibre-reinforced materials, J. Appl. Math. Phys. 39 (1988) 550–558.

[16] J.W. Hutchinson, H.M. Jensen, Models for fibre debonding and pullout in brittle composites with friction, Mech. Mater. 9 (1990) 139–163.